Identification of Agricultural Drought through Vegetation Health Analysis at Erap Station under the Markham Valley of Papua New Guinea

Samanta, S.
The Papua New Guinea University of Technology, Private Mail Bag, Lae, Morobe Province, Papua New Guinea, E-mail: rsgis.sailesh@gmail.com

DOI: https://doi.org/10.52939/ijg.v20i11.3691

Abstract
Drought is a phenomenon caused by insufficient soil moisture resulting from prolonged periods of low rainfall and the absence of proper irrigation systems. Its impact on crops, agricultural productivity, and the overall environment is significant. The use of multispectral satellite remote sensing data greatly facilitates the identification of agricultural drought. This study outlines a practical approach for assessing drought using multispectral satellite data. The main objective of this research is to estimate drought indicators and their relationship with ground conditions by analyzing remote sensing datasets through vegetation health index (VHI) analysis. The study is conducted at Erap, which is situated on the northern bank of the Markam River. Spectral bands, like near-infrared, red, and thermal bands of the Landsat 8 satellite are used to produce the VHI database. Multispectral data from the Landsat 8 satellite is the key dataset used to calculate the normalized differential vegetation index (NDVI) and land surface temperature (LST). The vegetation condition index (VCI) and temperature condition index (TCI) are derived from NDVI and LST, respectively. Ultimately, the VHI is calculated by combining VCI and TCI. The resulting VHI varies from 8 to 87, where the lower VHI values refer to extreme drought conditions and higher values denote normal conditions. Mild to moderate drought conditions were observed in the central and some areas in the western part of the research area. The R^2 between NDVI and VHI is calculated higher (0.72) compared to LST and VHI (0.40). The research indicates that multispectral satellite data is highly beneficial in predicting agricultural drought in any region based on temperature and vegetation conditions. VHI has the potential to be utilized in scientific contexts across different fields, particularly in agriculture and land use planning.

Keywords: Drought, Land Surface Temperature, Normalized Differential Vegetation Index, Temperature Condition Index, Vegetation Condition Index, Vegetation Health Index

1. Introduction

The fluctuation of moisture levels in the topsoil or underlying soil is attributed to minimal or absent precipitation and elevated temperatures over a specific timeframe [1]. Drought can be defined as a deficiency in soil moisture compared to its typical state [2]. The agricultural industry relies heavily on weather patterns, climate, and soil conditions. Agricultural drought adversely affects crop yield due to unfavorable soil moisture conditions caused by erratic rainfall and rising surface temperatures in non-irrigated regions [3]. The Asia-Pacific region experiences an average annual loss of US$404 billion due to vegetation drought, which corresponds to around 1.4% of the gross domestic product of this region [4]. The rise in meteoritical drought frequency, duration, and intensity is largely attributed to rapid anthropogenic activities and global warming trends [5]. As a result, the establishment of a regular and continuous drought monitoring system is imperative for sustainable growth in the agricultural domain. Traditionally, drought monitoring relied on in situ measurements of parameters responsible for drought [6]. Different conventional methods like the standardized precipitation index and Palmer drought severity index are used for assessing meteorological drought, which relies on imprecise station data rather than considering factors such as heat stress on vegetation growth, land use, and land cover, or vegetation characteristics [7] [8] and [9]. However, the advent of remote sensing has revolutionized the field, enabling the observation and estimation of critical drought-related parameters on a broader spatial and temporal scale [2] and [10].

It is much more difficult to observe the drought conditions on foot in larger plantation areas. The eye on the sky is an alternative in this case, which can save time and reach the blind area on a vast farm area. Multispectral satellite data acquired through a remote sensing process are very helpful in identifying the drought conditions in an agriculture-dominated area. Researchers have utilized various comprehensive monitoring indicators to evaluate drought conditions through satellite remote sensing data, such as the precipitation condition index [11], optimized meteorological drought index [12], soil moisture condition index [13], vegetation health index [14], etc. The vegetation health index (VHI) is a widely used method that effectively captures drought characteristics by considering both temperature and vegetation information [15]. The calculation of VHI depends on two factors, namely the vegetation condition index [16] and the temperature condition index [17]. These factors can be derived from the normalized differential vegetation index (NDVI) [18] and land surface temperature (LST) [19]. The fundamental concept behind VHI is to indicate inadequate vegetation health through a combination of low NDVI and high LST values, while conversely, optimal vegetation health is represented by higher NDVI values and lower LST values [20]. The major three objectives of this study are to (a) carry out TCI analysis based on thermal satellite-driven land surface temperature, (b) perform VCI analysis based on NDVI, and finally (c) conduct the VHI analysis to identify and monitor the health and growth condition of the plantation.

2. Methodology

2.1 Study Location

Erap and its surrounding area, which is situated on the northern bank of the Markham River is selected to conduct agricultural drought assessment. It spans from 146º 35′ 05″ E to 146º 42′ 15″ E longitude and 6º 31′ 50″ S to 6º 38′ 15″ S latitude, bordered by the Rumu River to the west and the Erap River to the east (Figure 1) within the Morobe province of Papua New Guinea. The primary land use and land cover in this region is agriculture, with a focus on Palm oil plantations, rice cultivation, and sparse vegetation. The majority of soils in the area are moderately well-drained. The climate is classified as tropical rainforest (Koppen climate classification: Af), with an average annual rainfall of 1750 mm and an average temperature of 22 degrees Celsius. December is typically warm, while July is cooler. The Markham Valley experiences significant climate variations each year due to the El Niño-Southern Oscillation. Furthermore, a decline in soil moisture levels has been noted due to decreased precipitation. As a result, crop productivity is significantly affected, requiring farmers to implement moisture-conserving techniques in these conditions.

2.2 Materials Used

The primary reliance of the research is on the multispectral satellite image captured by Landsat 8. The Landsat 8 satellite mission offers moderate spatial resolution (15 m to 100 m) datasets of the Earth's terrestrial areas. These measurements cover various spectrums including visible, near-infrared, short-wave infrared, and thermal infrared. All nine spectral bands from the operational land imager (OLI) and two spectral bands from a thermal infrared sensor (TIRS) are obtained from Earth Explorer (https://earthexplorer.usgs.gov/). This satellite data was collected on a clear day (03.03.2014) and is free from clouds or aerosols. The multispectral image is formed by combining all the bands using the layer stack process. The data is rectified using the Universal Transverse Mercator (UTM) coordinate system. The image underwent geometric correction with an accuracy of ±0.25 pixels. Subsequently, the image is cropped with the study area boundary to fit the study area for further analysis. Detailed information about each band and their respective spatial resolutions can be found in Table 1. The spatial resolution of OLI bands is 30m. Although the actual spatial resolution of the TIRS bands is 100m, the dataset is resampled to 30m by the data providers for level-1 product processing.

2.3 Calculation of NDVI and LST

Drought conditions are assessed using two geospatial parameters, namely the NDVI and LST. These parameters are obtained by analyzing the near-infrared band (5^{th} band), red band (4t band), and thermal band (10^{th} band) of Landsat 8 satellite imagery. The NDVI index measures the level of greenness in vegetation, providing valuable information about vegetation density and changes in plant health [18]. NDVI is calculated by subtracting the near-infrared from the red band and dividing the result by the sum of the NIR and Red bands. On the other hand, land surface temperature indicates the amount of heat present on the land when touched [21]. The temperature data is predominantly established by analyzing the thermal bands of the thermal remote sensing procedure [22].

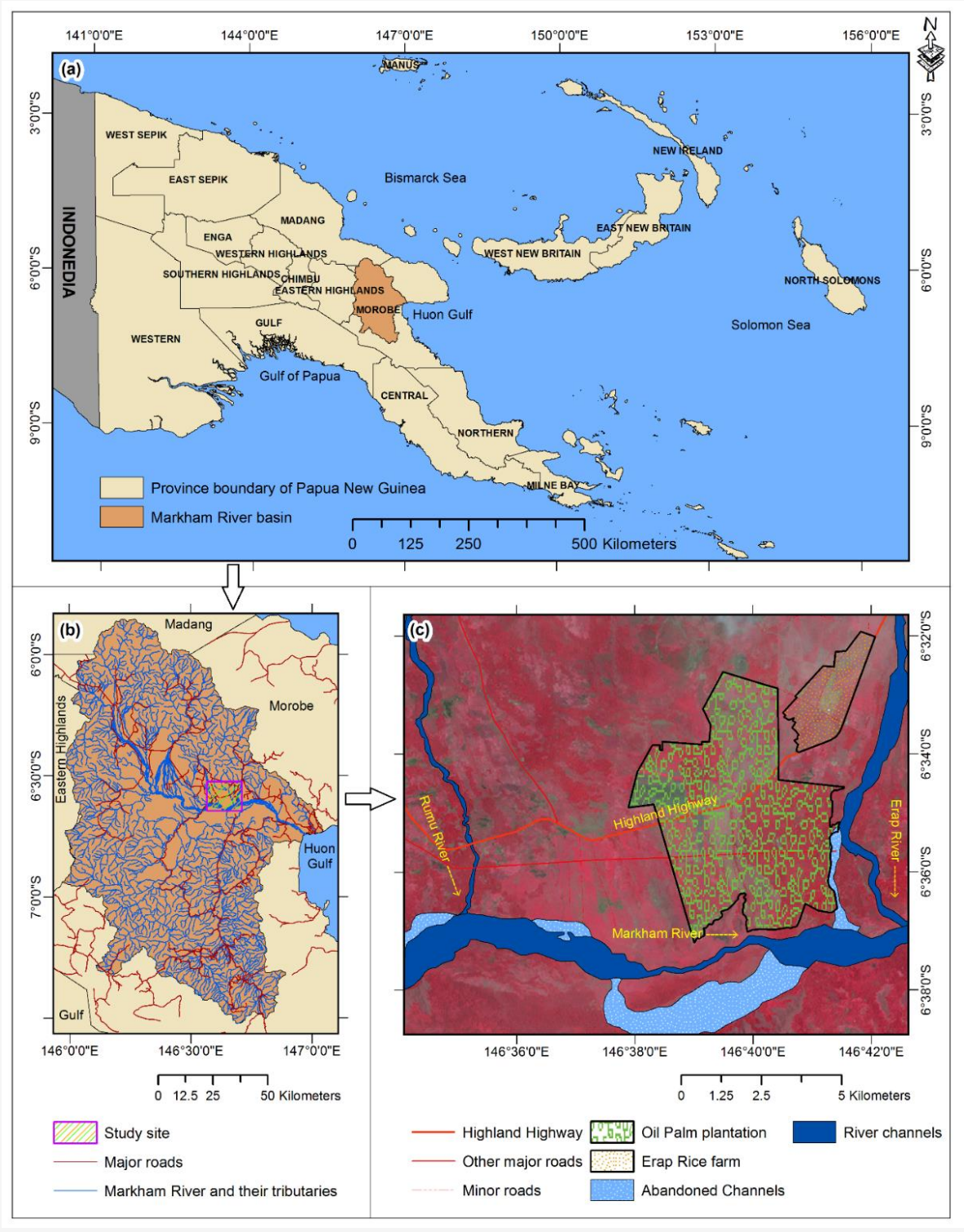

Figure 1: The locality map of the study area
(a) Provinces of Papua New Guinea with Markham watershed location
(b) The geographical location of Markham River basin with drainage and major road network
(c) The standard false color composite view of the study area image with river, road, and agricultural boundary

Table 1: Details of multispectral bands of Landsat 8 satellite image

Band numbers	Band	Spectral bandwidth (µm)	Spatial resolution (m)
1	Coastal Aerosol	0.43 to 0.45	30
2	Blue	0.450 to 0.51	30
3	Green	0.53 to 0.59	30
4	Red	0.64 to 0.67	30
5	Near-Infrared	0.85 to 0.88	30
6	Short-wave Infrared 1	1.57 to 1.65	30
7	Short Wave Infrared 2	2.11 to 2.29	30
8	Panchromatic	0.50 to 0.68	15
9	Cirrus	1.36 to 1.38	30
10	Thermal Infrared 1	10.6 to 11.19	30 (resampled)
11	Thermal Infrared 2	11.5 to 12.51	30 (resampled)

To derive NDVI and LST from OLI and TIRS bands, a series of calculations are performed, including the extraction of spectral radiance value (Equation 1), calculation of brightness temperature (Equation 2), calculation of NDVI (Equation 3), determination of vegetation proportion (Equation 4), calculation of land surface emissivity (Equation 5), and finally obtaining the land surface temperature (Equation 6) [18] [19] [21] and [22].

$$L_\lambda = 0.1 + 0.0003342 Q_{cal}$$

Equation 1

$$BT = \left[\frac{1321.0789}{\ln\left(\frac{774.8853}{L_\lambda}\right)+1} - 273.15 \right]$$

Equation 2

$$NDVI = \frac{NIR - RED}{NIR + RED}$$

Equation 3

$$P_v = \left[\frac{NDVI - NDVI_{\min}}{NDVI_{\max} - NDVI_{\min}} \right]^2$$

Equation 4

$$\varepsilon = 0.004Pv + 0.986$$

Equation 5

$$LST = \left[\frac{BT}{1+\left(0.00115\frac{BT}{1.4388}\right)ln(\varepsilon)} \right]$$

Equation 6

Where L_λ refers to the atmospheric (top) spectral radiance, 0.0003342 is the band-specific multiplicative rescaling factor, 0.1 is the band-specific rescaling factor, Qcal represents the pixel value of band 10, *BT* stands for the brightness temperature,774.8853 and 1321.0789 are the band-specific thermal conversion constants, P_v stands for the proportion of vegetation, ε represents the land surface emissivity and *LST* is land surface temperature.

2.4 Calculation of VCI, TCI, and VHI

The agricultural drought index is calculated using the VHI model, which combines the VCI and TCI indices [23]. Both the TCI and VCI indices are computed using multispectral satellite data, but they utilize different observation inputs. The VCI incorporates information from the visible and near-infrared parts of the spectrum and is derived from the NDVI [24]. On the other hand, the TCI calculation involves the use of LST, which is obtained from thermal bands [25]. All the necessary data are derived from Landsat 8, a medium-resolution multispectral satellite image. The VHI is derived through three consecutive calculations, as presented in equations 7 to 9 [16] [17] [23] [24] and [25]. The overall methodological flow chart in the estimation of drought conditions is presented in Figure 2.

$$VCI = \left[\frac{NDVI - NDVI_{\min}}{NDVI_{\max} - NDVI_{\min}} \right] \times 100$$

Equation 7

$$\mathrm{TCI} = \left[\frac{\mathrm{LST}_{\min} - \mathrm{LST}}{\mathrm{LST}_{\max} - \mathrm{LST}_{\min}} \times 100 \right]$$

Equation 8

$$VHI = 0.5[VCI + TCI]$$

Equation 9

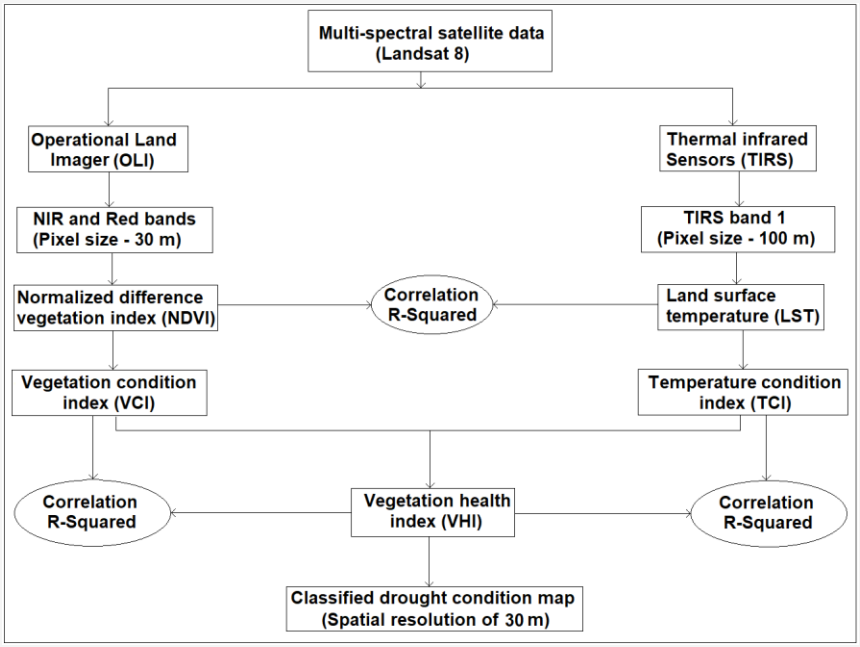

Figure 2: The overall methodological flow chart in the estimation of drought condition

Where VCI represents the vegetation condition index, NDVI stands for normalized differential vegetation index, TCI represents the temperature condition index, VHI stands for vegetation health index, and 0.5 is a coefficient value that regulates the combinations of the VCI and the TCI to the VHI [26].

3. Results and Discussion

NDVI characterizes the phenology of vegetation, with positive values indicating healthy and dense vegetation, and negative values representing water and wetland areas. The range of NDVI ranges from -0.551 to 0.627 (Figure 3(a)). Negative NDVI values are observed in the active river channel, abandoned river channels, and certain pockets in the middle, as well as in the northern section of the study site. Conversely, higher NDVI values are found in the east, southeast, and north sections of the study area indicating a prevalence of plantation and vegetation. The modeled land surface temperature (LST) in this area varies from 7º to 39º Celsius (C). Some sections in the east, northwest, and middle sections of the study site experience the highest temperatures. On the other hand, a linear zone stretching from the northeast corner to the southwest portion exhibits the lowest temperature (Figure 3(b)). The calculated VCI values ranged between 20.88 and 83.43 (Figure 3(c)). Lower VCI values represent poor vegetation conditions found over the active and abandoned river channel and some pockets in the middle and north sides of the research location. Alternatively, high VCI values represent good vegetation conditions observed in the east, southeast, and north sections. The modeled TCI in this region ranges from 32.76 to 87.93. The eastern part, along with certain areas in the central and northwest regions, experiences the minimum temperature conditions, while a linear zone extending from the northeast corner to the southwest portion is characterized by high-temperature conditions (Figure 3(d)).

This research utilizes the VHI, a holistic measure that merges the VCI and TCI, with a scale from 0 (severe dryness) to 100 (ideal moisture) [27]. In this study, the VCI output ranged from 8 to 87. The complete range is divided into seven categories, where the initial three categories indicated no drought conditions, specifically (i) excellent (> 60), (ii) good (50 - 60), and (iii) normal (40 - 50). The remaining categories are classified as (iv) mild dry (30 – 40), (v) moderately dry (20 - 30), (vi) severely dry (10 - 20), and (vii) extremely dry (< 10). In the research area, mild drought conditions are observed in the central region as well as certain areas in the western part (Figure 4). The current position of the rice farm and a significant portion of the oil palm plantation are typically unaffected by drought conditions. However, the western part of the oil palm plantation is facing varying degrees of drought, ranging from mild to moderate. This section of the oil palm plantation is disturbed by man-made structures and farm buildings. The utilization of Landsat 8 remote sensing data in this study demonstrates that VHI has the potential to monitor drought in the Markham Valley region effectively.

The VHI value is quantified in percentages from 1 to 100. When the VHI falls below 40, vegetation stress can be anticipated indicating potential crop and pasture production losses. Conversely, indices above 60 signify robust and healthy vegetation. VHI is derived through VCI and TCI obtained from satellite image-driven NDVI and LST. NDVI is sensitive and changes with the fluctuation of soil moisture levels in an agriculture zone [28].

VCI range from 50 to 100 signifies vegetation conditions above normal, while values falling between 50 and 35 indicate drought conditions and anything below 35 indicates a severe drought situation. LST generally decreases as surface soil moisture increases, except in high-latitude areas [29]. The TCI may range from 0, indicating extremely unfavorable conditions, to 100, representing optimal conditions.

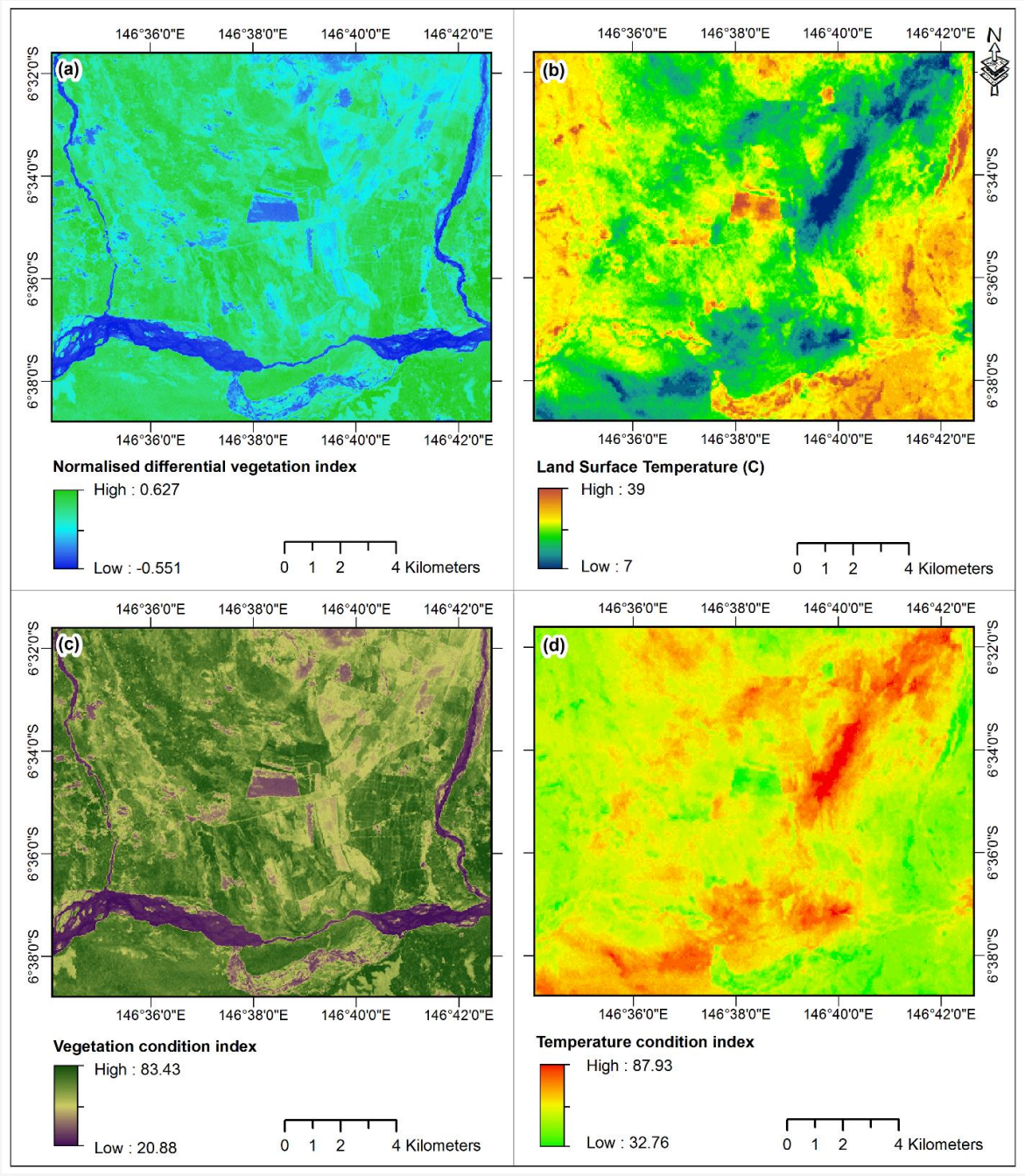

Figure 3: Spectral indices (a) NDVI (b) LST (c) VCI (d) TCI

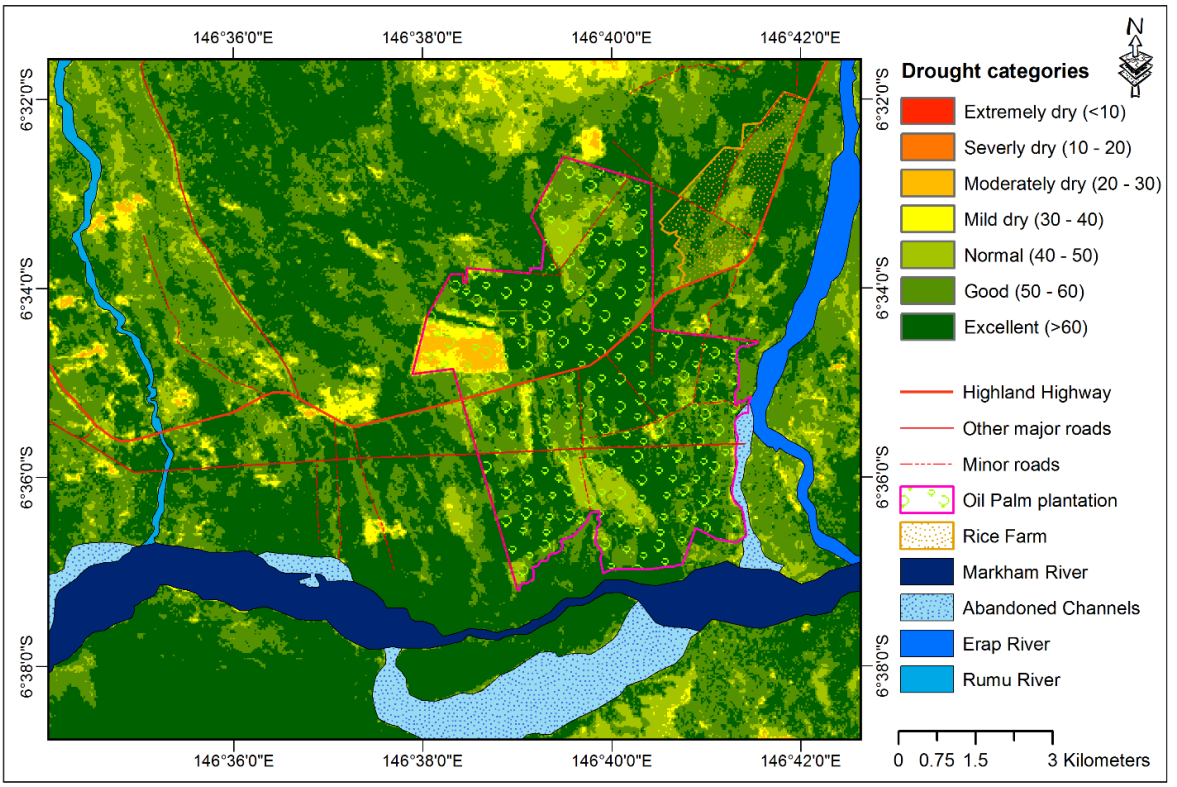

Figure 4: Drought severity derived from NDVI-based VCI and LST-based TCI

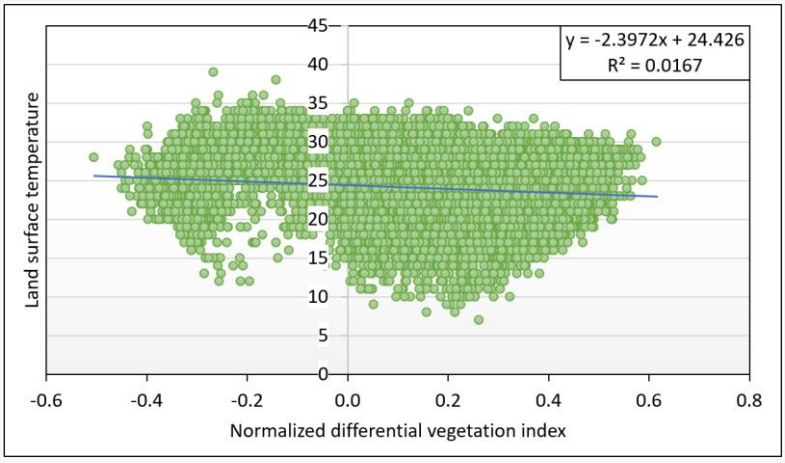

Figure 5: Correlation between NDVI and LST

TCI is employed to assess the impact of temperature and excessive moisture on vegetation stress. The research examined the connection between NDVI and LST using linear regression analysis, uncovering a mild inverse correlation (R^2 of 0.02) where surface temperature increases as vegetation index decreases (Figure 5). A strong positive coefficient of determination (R^2 of 0.72) is computed between NDVI and VHI, indicating that the normalized differential vegetation index is the major factor in assessing vegetation health. On the other hand, a moderately strong negative correlation (R^2 of 0.40) is computed between LST and VHI, indicating that the vegetation health decreases with the increase in surface temperature. Figure 6 represents the coefficient of determination between NDVI-VHI and LST-VHI. The spatial resolution of the VHI output is generated in a 30m pixel size, which is similar to the spatial resolution of OLI and resamples TIRS bands.

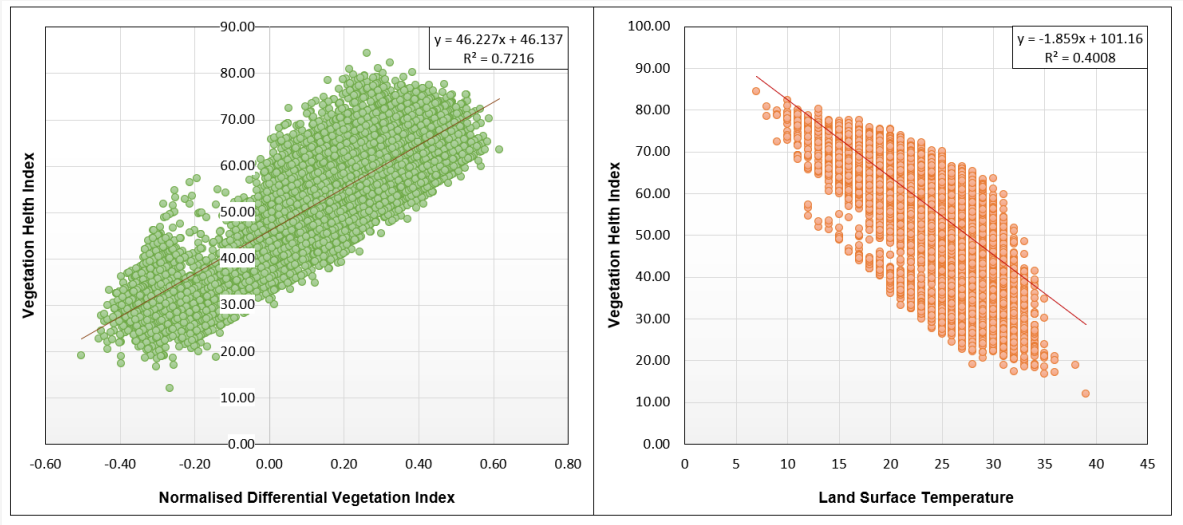

Figure 6: Correlation between NDVI-VHI, and LST-VHI feature space

4. Conclusions

The findings of this research highlight the significant benefits of multispectral satellite data in predicting agricultural drought in any given area, by analyzing temperature and vegetation conditions. VCI is created using the NDVI database and the TCI from the LST database. The calculation of NDVI involves comparing the near-infrared (NIR) and red (R) band pixel values of Landsat 8 satellite data. On the other hand, the LST is driven from the thermal band (10^{th}) and incorporation of NDVI through several equations (equations 1 through 6). A strong positive correlation (R^2 of 0.72) is observed between NDVI and VHI, compared to LST and VHI (R^2 of 0.40). This indicates that NDVI is the major influencing factor in assessing vegetation health. Medium spatial resolution data, like 30m OLI datasets provides more details and better spatial accuracy than broad-scale data of 100m TIRS bands of Landsat 8 series satellite images. However, as per metadata information, the data providers supplied the TIRS bands after resampling to 30m spatial resolution for level-1 product processing. The findings indicated that VHI has the potential to be utilized in scientific contexts across different fields, particularly in agriculture and land use planning. Spatial drought databases are effectively employed for analyzing watersheds, studying water balance, assessing soil respiration, examining hydrology, monitoring soil health, evaluating plant growth, measuring plant water stress, and scheduling irrigation. Both the VCI and the TCI are significant in the calculation of VHI, although they can be influenced by various climatic and environmental variables, which are not considered in this case study. Given the variations in environmental conditions across different regions, assigning equal importance to VCI and TCI could potentially limit the effectiveness of VHI applications, leading to heightened uncertainty in drought identification. It is important to note that the calculation of VHI does not directly incorporate the precipitation factor. The VHI provides an accurate depiction of the drought situation and serves as a proxy for assessing crop conditions. Although it is recommended to establish comprehensive ground-based models, a satellite-based drought model can be used to generate accurate and dependable drought information systems for both immediate and prolonged timeframes for large catchment areas with the inclusion of satellite-based precipitation data. Further research is suggested with the inclusion of rainfall and soil moisture data, which will take care of the precipitation factor and will improve the accuracy. Additionally, the use of high-resolution multispectral satellite data will enhance the certainty of prediction.

References

[1] Yuan, Y., Ye, X., Liu, T. and Li, X., (2023). Drought Monitoring Based on Temperature Vegetation Dryness Index and Its Relationship with Anthropogenic Pressure in a Subtropical Humid Watershed in China, *Ecological Indicators,* Vol. 154. https://doi.org/10.1016/j.ecolind.2023.110584.

[2] West, H., Quinn, N. and Horswell, M., (2019). Remote Sensing for Drought Monitoring & Impact Assessment: Progress, Past Challenges and Future Opportunities. *Remote Sensing of Environment*, Vol. 232. https://doi.org/10.1016/j.rse.2019.111291.

[3] Krueger, E. S., Ochsner, T. E. and Quiring, S. M., (2019). Development and Evaluation of Soil Moisture-Based Indices for Agricultural Drought Monitoring. *Agronomy Journal*, Vol. 111(3), https://doi.org/10.2134/agronj2018.09.0558.

[4] Wu, B., Ma, Z. and Yan, N., (2020). Agricultural Drought Mitigating Indices Derived from the changes in Drought Characteristics. *Remote Sensing of Environment*, Vol. 244. https://doi.org/10.1016 /j.rse.2020.111813.

[5] Chiang, F., Mazdiyasni, O. and AghaKouchak, A., (2021). Evidence of Anthropogenic Impacts on Global Drought Frequency, Duration, and Intensity. *Nature Communications*, Vol. 12(1), https://doi.org/10.1038/s41467-021-22314-w.

[6] Zhang, R., Wu, X., Zhou, X., Ren, B., Zeng, J. and Wang, Q., (2022). Investigating the Effect of Improved Drought Events Extraction Method on Spatiotemporal Characteristics of Drought. *Theoretical and Applied Climatology*, Vol. 147. https://doi.org/10.1007/s00704-021-03838-z.

[7] Hayes, M. J., Svobod, M. D., Wardlow, B. D., Anderson, M. C. and Kogan, F., (2012). Drought Monitoring: Historical and Current Perspectives. *Drought Mitigation Center Faculty Publications*, CRC Press, 1-19. http://digitalcommons.unl.edu/droughtfacpub/94.

[8] Dabanli, I., Mishra, A. K. and Sen, Z., (2017). Long-term Spatio-Temporal Drought Variability in Turkey. *Journal of Hydrology*, Vol. 552. https://doi.org/10.1016/j.jhydrol.2017.07.038.

[9] Rimkus, E., Stonevicius, E., Kilpys, J., Maciulyte, V. and Valiukas, D., (2017). Drought Identification in The Eastern Baltic Region Using NDVI. *Earth System Dynamics*, Vol. 8(3). https://doi.org/10.5194/esd-8-627-2017.

[10] Alahacoon, N. and Edirisinghe, M., (2022). A Comprehensive Assessment of Remote Sensing and Traditional Based Drought Monitoring Indices at Global and Regional Scale. *Geomatics, Natural Hazards and Risk*, Vol. 13(1). https://doi.org/10.1080/19475705.2022.2044394.

[11] Du, L., Tian, Q., Yu, T., Meng, Q., Jancso, T., Udvardy, P. and Huang, Y., (2013). A Comprehensive Drought Monitoring Method Integrating MODIS and TRMM Data. *International Journal of Applied Earth Observation and Geoinformation*, Vol. 23. https://doi.org/10.1016/j.jag.2012.09.010.

[12] Wei, W., Zhang, J., Zhou, J., Zhou, L., Xie, B. and Li, C., (2021). Monitoring Drought Dynamics in China using Optimized Meteorological Drought Index (OMDI) Based on Remote Sensing Data Sets. *Journal of Environmental Management*, Vol. 292. https://doi.org/10.1016/j.jenvman.2021.112733

[13] Hwang, T. H., Kim, B. S., Kim, H. S. and Seoh, B. H., (2006). The Estimation of Soil Moisture Index by SWAT Model and Drought Monitoring. *KSCE Journal of Civil and Environmental Engineering Research*, Vol. 26(4B). https://doi.org/10.12652/Ksce.2006.26.4B.345.

[14] Bento, V. A., Gouveia, C. M., DaCamara, C. C. and Trigo, I. F., (2018). A Climatological Assessment of Drought Impact on Vegetation Health Index. *Agricultural and Forest Meteorology*, Vol. 259. https://doi.org/10.1016/j.agrformet.2018.05.014.

[15] Bento, V. A., Gouveia, C. M., DaCamara, C. C., Libonati, R. and Trigo, I. F., (2020). The Roles of NDVI and Land Surface Temperature when using the Vegetation Health Index Over Dry Regions. *Global and Planetary Change*, Vol. 190. https://doi.org/10.1016/j.gloplacha.2020.103198.

[16] Jiao, W., Zhang, L., Chang, Q., Fu, D., Cen, Y. and Tong, Q., (2016). Evaluating an Enhanced Vegetation Condition Index (VCI) Based on VIUPD for Drought Monitoring in the Continental United States. *Remote Sensing*, Vol. 8(3). https://doi.org/10.3390/rs8030224.

[17] Tian, M., Wang, P. and Khan, J., (2016). Drought Forecasting with Vegetation Temperature Condition Index Using ARIMA Models in the Guanzhong Plain. *Remote Sensing*, Vol. 8(9). https://doi.org/10.3390/rs8090690.

[18] Jagtap, A., Shedge, D., and Mane, P. (2024). Exploring the Effects of Land Use/Land Cover (LULC) Modifications and Land Surface Temperature (LST) in Pune, Maharashtra with Anticipated LULC for 2030. *International Journal of Geoinformatic*s, Vol. 20(2), 42–63. https://doi.org/10.52939/ijg.v20i2.3065.

[19] García-Santos, V., Cuxart, J., Martínez-Villagrasa, D., Jiménez, M. A. and Simó, G., (2018). Comparison of Three Methods for Estimating Land Surface Temperature from Landsat 8-Tirs Sensor Data. *Remote Sensing*, Vol. 10(9). https://doi.org/10.3390/rs10091450.

[20] Yousef, F., Gebremichael, M., Ghebremichael, L. and Perine, J., (2019). Remote-Sensing Based Assessment of Long-term Riparian Vegetation Health in Proximity to Agricultural Lands with Herbicide Use History. *Integrated Environmental Assessment and Management*, Vol. 15, https://doi.org/10.1002/ieam.4144.

[21] Sharaf El Din, E., Elsherif, A., Ramadan, S., and Aboelkhair, H. (2023). Mapping of Thermal Indices Using an Automated Landsat 8-based-ArcGIS Model: A Case Study in Alexandria City, Egypt. *International Journal of Geoinformatic*s, Vol. 19(9), 1–12. https://doi.org/10.52939/ijg.v19i9.2823.

[22] Thammaboribal, P. (2024). Investigating Land Surface Temperature Variation and Land Use Land Cover Changes in Pathumthani, Thailand (1997-2023) using Landsat Satellite Imagery: A Comprehensive Analysis of LST and Urban Hot Spots (UHS). *International Journal of Geoinformatics*, Vol. 20(2), 27–41. https://doi.org/10.52939/ijg.v20i2.3063.

[23] Gidey, E., Dikinya, O., Sebego, R., Segosebe, E. and Zenebe, A., (2018). Analysis of the Long-Term Agricultural Drought Onset, Cessation, Duration, Frequency, Severity and Spatial Extent using Vegetation Health Index (VHI) in Raya and its Environs, Northern Ethiopia. *Environmental Systems Research*, Vol. 7, https://doi.org/10.1186/s40068-018-0115-z.

[24] Thavorntam, W. and Shahnawaz. (2022). Evaluation of Drought in the North of Thailand using Meteorological and Satellite-Based Drought Indices. *International Journal of Geoinformatics*, Vol. 18(5), 13–26. https://doi.org/10.52939/ijg.v18i5.2367.

[25] Gaikwad, S. V., Kale, K. V., Dhumal, R. K. and Vibhute, A. D., (2015). Analysis of TCI Index using Landsat8 TIRS Sensor Data of Vaijapur Region. *International Journal of Computer Sciences and Engineering*, Vol. 3(8), 60-64.

[26] Rojas, O., Vrieling, A. and Rembold, F., (2011). Assessing Drought Probability for Agricultural Areas in Africa with Coarse Resolution Remote Sensing Imagery. *Remote Sensing of Environment*, Vol. 115(2). https://doi.org/10.1016/j.rse.2010.09.006.

[27] Aitekeyeva, N., Li, X., Guo, H., Wu, W., Shirazi, Z., Ilyas, S., Yegizbayeva, A. and Hategekimana, Y., (2020). Drought Risk Assessment in Cultivated Areas of Central Asia using MODIS Time-Series Data. *Water*, Vol. 12(6). https://doi.org/10.3390/w12061738.

[28] Ahmad, S., Kalra, A. and Stephen, H., (2010). Estimating Soil Moisture Using Remote Sensing Data: A Machine Learning Approach. *Advances in Water Resources*, Vol. 33(1), https://doi.org/10.1016/j.advwatres.2009.10.008.

[29] Ghahremanloo, M., Mobasheri, M. R. and Amani, M., (2019). Soil Moisture Estimation using Land Surface Temperature and Soil Temperature At 5 cm Depth. *International Journal of Remote Sensing*, Vol. 40(1). https://doi.org/10.1080/01431161.2018.1501167.